Kinematics Analysis of 4-RPUR Parallel Mechanism with 3D Rotation Center Overlap for Ankle Rehabilitation

Xiangyu Shen, Hongjian Yu* and Zhenyi Wang
State Key Laboratory of Robotics and Systems, Harbin Institute of Technology, Harbin, China

Keywords: Less DOF Parallel Mechanism, Ankle Rehabilitation Robot, Kinematics Analysis.

Abstract: In many robot application environments, there are often requirements for the three-dimensional rotation center of the robot operating platform to coincide, such as the design of the robot wrist, the design of the robot to assist the human joint movement, etc. However, in the research and development of parallel robots with few degrees of freedom, It is difficult to design a mechanism that can rotate the robot's moving platform around a fixed point with limited degrees of freedom. The main content of this paper is the kinematic analysis and discussion of a 4-RPUR parallel configuration that can realize three-dimensional rotation around a certain point in space and the design of a reset rehabilitation robot based on this configuration.

1 INTRODUCTION

The parallel mechanism with higher stiffness and stronger bearing capacity is used for ankle joint rehabilitation robots. With the development of parallel mechanisms, the parallel configuration has been applied more rapidly in rehabilitation robots. In the late 20th century, Rutgers University in the United States proposed the "Rutgers Ankle" for ankle rehabilitation training. The system is based on the Stewart configuration, which is the first application of parallel mechanisms in medical rehabilitation structures (Girone M, 2001). Later, Yooh and Ryu in South Korea proposed a gas-powered ankle rehabilitation system with four degrees of freedom, which uses two parallel mechanisms to realize the movement of the moving platform in three directions. It can also achieve the relative rotation of the front foot and the back foot of the affected foot (Kaufman KR, 1996). Fan Xiaoqin et al from the North University of China proposed a (2-SPS+PU)&R hybrid ankle joint rehabilitation robot. Based on the theory of traditional Chinese medicine treatment, this configuration can realize a complete three-degree of freedom rotation of the ankle joint and movement along the tibia (Fan X, 2019). Then, Liu Chenglei et al. (Liu C, 2021) proposed a parallel mechanism for ankle joint rehabilitation. Based on the U_1U_2 ankle base fitting model, this scheme is a four-degree-of-freedom generalized spherical mechanism, which reduces the human-computer interaction force caused by the ball-hinge motion model in the rehabilitation process. At the same time, Han Yali et al. (Han Y L, 2015) proposed a 3-RUPS/S configuration of a 3-DOF parallel robot. In addition, there are 3-RSS/S, 3-PSS/S, and 4-SPS/S configurations with the same principle, which are characterized by the central pillar restraining excess mobility degrees of freedom (Liu G Q, Zhao T S). Yu Runtian et al (Yu R T, 2015), Zhang et al (Zhang X J, 2006), and Shiping Zuo et al (Zuo S P, 2020) studied 3-DOF ankle joint rehabilitation robots, but most of the robots developed had poor reset function due to lack of freedom.

2 DESCRIPTION OF ROBOT MECHANISM

2.1 Mechanism Modeling of 4-RPUR

The motion principle model of the ankle joint rehabilitation robot proposed in this paper based on the 4-RPUR configuration is shown in Figure 1. The robot configuration has four limbs. This section analyzes its configuration characteristics and constraint characteristics. The four degrees of freedom of the structure can meet the requirements of rehabilitation and traction reset. At the same time, the rotation center of the mechanism is in the center of the mechanism, and the spatial position of the rotation

Shen, X., Yu, H. and Wang, Z.
Kinematics Analysis of 4-RPUR Parallel Mechanism with 3D Rotation Center Overlap for Ankle Rehabilitation.
DOI: 10.5220/0012275900003807

In *Proceedings of the 2nd International Seminar on Artificial Intelligence, Networking and Information Technology (ANIT 2023)*, pages 131-137
ISBN: 978-989-758-677-4

center is related to the intersection points of the fourth and fifth rotation auxiliary axes of each limb. It is only necessary to design the adjusting mechanism to change the relative position of the installation ring of the fixed foot and the intersection point to meet the different installation positions. Adaptation of rotation centers for different foot sizes.

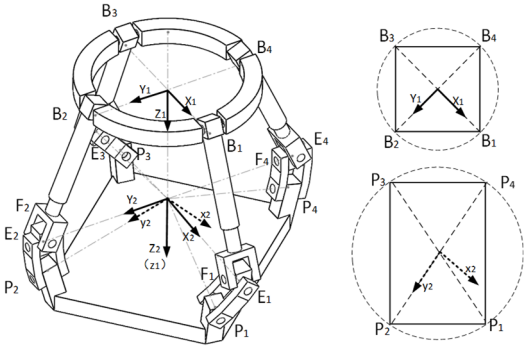

Figure 1: 4-RPUR parallel robot and hinge arrangement of the moving and fixed platform.

In Figure 1, B_1-B_4 points are the center positions of the rotation axis connected by the fixed platform; P_1-P_4 points are rotating sub-center points connected with the moving platform; The coordinates of the rotation centers of the four Hooke hinges are denoted as E_1-E_4, F_1-F_4, respectively. The platform is a square, whose four vertices are B_1, B_3, B_3, and B_4; The moving platform is a rectangle with four vertices P_1, P_2, P_3, and P_4.

The coordinate system of the robot is established as shown in Figure 1, in which the base coordinate system O_1-$X_1Y_1Z_1$, the coordinate origin is at the center point of the top platform (fixed platform), and X_1 and B_1B_3 are in the same direction. The coordinate origin o1 of the moving coordinate system o_1-$x_1y_1z_1$ is located at the junction point of the fourth and fifth rotation axes of the limb calculated from the fixed platform. The z_1 axis is completely perpendicular to the robot's moving platform, and the positive direction is toward the moving platform. We also need to establish an additional reference coordinate system O_2-$X_2Y_2Z_2$, whose origin coincides with the moving coordinate system o_1, its X_2 axis is parallel to and in the same direction as the base coordinate system X_1 axis, and its Z_2 is in the same direction as the moving coordinate system z_1.

According to the established coordinate system, it is easy to obtain: From fixed platform to moving platform, write the motion screw of the four limbs in the reference coordinate system O_2-$X_2Y_2Z_2$:

$$\left(\$_{i1}\ \ \$_{i2}\ \ \$_{i3}\ \ \$_{i4}\ \ \$_{i5}\right)=\begin{pmatrix}0 & 0 & 0 & l_{i4} & l_{i5}\\ 1 & 0 & 1 & 0 & m_{i5}\\ 0 & 0 & 0 & n_{i4} & n_{i5}\\ a_{i1} & l_{i2} & a_{i3} & 0 & 0\\ 0 & 0 & 0 & 0 & 0\\ c_{i1} & n_{i2} & c_{i3} & 0 & 0\end{pmatrix},i=1,3 \quad (1)$$

$$\left(\$_{i1}\ \ \$_{i2}\ \ \$_{i3}\ \ \$_{i4}\ \ \$_{i5}\right)=\begin{pmatrix}1 & 0 & 1 & 0 & l_{i5}\\ 0 & 0 & 0 & m_{i4} & m_{i5}\\ 0 & 0 & 0 & n_{i4} & n_{i5}\\ 0 & 0 & 0 & 0 & 0\\ b_{i1} & m_{i2} & b_{i3} & 0 & 0\\ c_{i1} & n_{i2} & c_{i3} & 0 & 0\end{pmatrix},i=2,4 \quad (2)$$

2.2 Freedom Analysis

It can be seen that first, the six moving screws included in the three-limb are linearly independent, so the first three-limb reciprocal screw can be obtained

$$\$_i^r=\left(0\ \ 1\ \ 0;\ \ 0\ \ 0\ \ 0\right),i=1,3 \quad (3)$$

This reciprocal screw restricts the motion of the moving platform in the direction of the base coordinate system Y_1;

By the same token, we can also obtain the second, four-limb reciprocal screw as:

$$\$_i^r=\left(1\ \ 0\ \ 0;\ \ 0\ \ 0\ \ 0\right),i=2,4 \quad (4)$$

This reciprocal screw restricts the movement of the moving platform in the direction of the base coordinate system X_1;

The constraint of the robot's four limbs on the moving platform is the constraint force vector in the $X_1O_1Y_1$ plane, which completely restricts the movement of the robot's rotation center along the X_1 axis and Y_1 axis of the base coordinate system. Therefore, this configuration loses the freedom of movement in both directions, and the relative position between the reference frame O_2-$X_2Y_2Z_2$ synchronous platforms is fixed, so it can also indicate that the robot has a definite coincident three-dimensional rotation center. The transformation of the constraint force vector to the base coordinates has the two largest linearly independent groups, so this configuration has two virtual constraints. The degrees of freedom of this configuration are calculated as follows:

$$M=d(n-g-1)+\sum_{g}^{i=1}f_i+I \quad (5)$$

In the above equation, d is the order of the mechanism, n is the Number of mechanism members, g is the Number of motion pairs, f_i is the Relative freedom of the pair, and I is the number of virtual constraints of the mechanism. The mechanism n=18, g=20, f_i=1 (i=1, 2, ... 20), according to the above analysis of the dynamic platform has no common

constraints, then λ=0. Mechanism d=6, but the virtual constraint is 2, then *I*=2, so the degree of freedom of the mechanism is *M*=60* (18-20-1) +20+2=4.

The basis of the four largest independent groups of reciprocal screws is:

$$\begin{cases} \$_i^r = (0 \quad 1 \quad 0 \quad 0 \quad 0 \quad 0) \\ \$_i^r = (1 \quad 0 \quad 0 \quad 0 \quad 0 \quad 0) \end{cases} \tag{6}$$

Because the moving platform can rotate around three axes and move along the Z direction, rigid motion pairs $\$_{12}$, $\$_{22}$, $\$_{32}$, and $\$_{42}$. Then each branch will add another reciprocal screw. The reciprocal screw fundamental solution system is obtained from the reciprocal product being zero:

Constraint screw system of the four limbs:

$$\begin{cases} \$_1^r = (0 \quad 1 \quad 0 \quad 0 \quad 0 \quad 0) \\ \$_2^r = \left(1 \quad 0 \quad \dfrac{(a_{i3}-a_{i1})}{(c_{i1}-c_{i3})}; 1 \quad -\dfrac{\left(l_{i5}-\dfrac{l_{i4}n_{i5}}{n_{i4}}\right)}{m_{i5}} \quad -\dfrac{l_{i4}}{n_{i4}} \right), i=1,3 \end{cases} \tag{7}$$

$$\begin{cases} \$_1^r = (1 \quad 0 \quad 0 \quad 0 \quad 0 \quad 0) \\ \$_2^r = \left(0 \quad 1 \quad \dfrac{(b_{i3}-b_{i1})}{(c_{i1}-c_{i3})}; -\dfrac{\left(m_{i5}-\dfrac{m_{i4}n_{i5}}{n_{i4}}\right)}{l_{i5}} \quad 1 \quad -\dfrac{m_{i4}}{n_{i4}} \right), i=2,4 \end{cases} \tag{8}$$

After rigidification, the resulting reciprocal screw $\$_{12}$ $\$_{22}$ $\$_{32}$ $\$_{42}$ linear independent, the reciprocal screw constraint of the moving platform is six linearly independent screws with no additional degrees of freedom. Therefore, the choice of input is reasonable.

3 ROBOT KINEMATICS ANALYSIS

The pose of the moving coordinate system o_1-$x_1y_1z_1$ is relative to the base coordinate system O_1-$X_1Y_1Z_1$ reflects the pose of the moving platform, namely, the Angle sx around the X_1 axis, the Angle sy around the Y1 axis, and the Angle sz around the Z1 axis, which are represented by the Euler Angle. The moving coordinate system o_1-$x_1y_1z_1$ relative to the base coordinate system O_1-$X_1Y_1Z_1$ can be represented by a transformation matrix:

$$[R] = \begin{bmatrix} c(sz)c(sy) & -s(sz)c(sx)+c(sz)s(sy)s(sx) & s(sz)s(sx)+c(sz)s(sy)c(ss) \\ s(sz)c(sy) & c(sz)c(sx)+s(sz)s(sy)s(sx) & -c(sz)s(sx)+s(sz)s(sy)c(sx) \\ -s(sy) & c(sy)s(sx) & c(sy)c(sx) \end{bmatrix} \tag{9}$$

The coordinate vector of point P in the moving coordinate system o_1-$x_1y_1z_1$ is:

$$\boldsymbol{P}_1^{'} = [151.66 \quad 26.74 \quad 41.26]^{\mathrm{T}}, \boldsymbol{P}_2^{'} = [0 \quad 154 \quad 41.26]^{\mathrm{T}}$$
$$\boldsymbol{P}_3 = [-151.66 \quad -26.74 \quad 41.26]^{\mathrm{T}}, \boldsymbol{P}_4^{'} = [0 \quad -154 \quad 41.26]^{\mathrm{T}} \tag{10}$$

The coordinates of the P point converted from the moving platform coordinates to the fixed platform are:

$$P_i = [R]P_i^{'} + O' \tag{11}$$

Among them $O' = [0 \quad 0 \quad h]$; h is the distance between the center of the moving platform coordinate system and the center of the base platform coordinate system. The coordinate vector of B in the fixed coordinate system O_1-$X_1Y_1Z_1$ is:

$$\boldsymbol{B}_1 = [95 \quad 0 \quad 0]^{\mathrm{T}}, \boldsymbol{B}_2 = [0 \quad 95 \quad 0]^{\mathrm{T}}, \boldsymbol{B}_3 = [-95 \quad 0 \quad 0]^{T}, \boldsymbol{B}_4 = [0 \quad -95 \quad 0]^{\mathrm{T}} \tag{12}$$

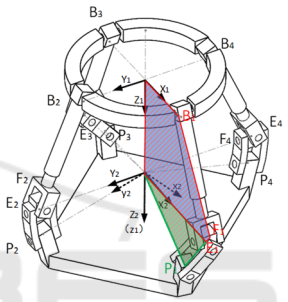

Figure 2: Robot inverse solution.

Analyze in the plane shown in Fig 2:

Let the coordinates of E_1 in a fixed coordinate system be:

$$E_1 = [a1 \quad 0 \quad b1]^{T} \tag{13}$$

Doing the same for the other limbs can get the equation as follow:

$$\begin{cases} |P_1E_1| = D \\ |E_1B_1| = R \end{cases} \begin{cases} |P_2E_2| = D \\ |E_2B_2| = R \end{cases} \begin{cases} |P_3E_3| = D \\ |E_3B_3| = R \end{cases} \begin{cases} |P_4E_4| = D \\ |E_4B_4| = R \end{cases} \tag{14}$$

Where *D* is the base length of the defined isosceles triangle, and *R* is the radius length of the defined isosceles triangle. The values of a_1, b_1, a_2, b_2, a_3, b_3, a_4, b_4 can be determined by the equation and the bar length constraints, and the coordinate vectors of points E_1, E_2, E_3, E_4 under O1-$X_1Y_1Z_1$ can be determined.

For the first limb, so far, we can determine the vectors $\boldsymbol{E_1o_1}$, $\boldsymbol{O_1o_1}$, and $\boldsymbol{O_1B_1}$.

The modular bias distance *e* of the vector $\boldsymbol{E_1F_1}$ can be obtained from the two-dimensional vector relation, the vertical relation between $\boldsymbol{E_1F_1}$ and $\boldsymbol{E_1o_1}$ can be obtained, and the coordinate vector of F_1 in the fixed coordinate system O_1-$X_1Y_1Z_1$ can be obtained.

Through the vector operation in the plane, it can be obtained that $B_1F_1=B_1O_1+O_1o_1+o_1E_1+E_1F_1$ and the change of B_1F_1 can be obtained, that is, the change of the moving pair of the first limb. In the same way, we can find the change in the motion pairs of the other three limbs.

The kinematics model of the robot is established by ADAMS, and a series of movements are carried out in the driving model under the initial state (sx=0°,sy=0°,sz=0°,h=160mm). The kinematics of the joint space in the ADAMS model is compared with the calculation results of the inverse kinematics derived in this paper, to verify the inverse kinematics model of the robot.

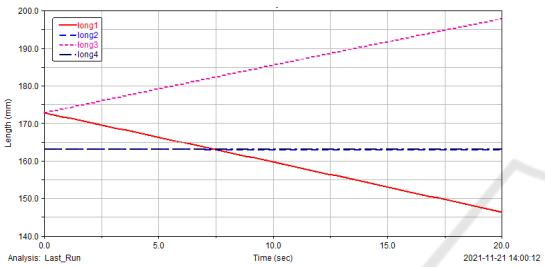

(a)

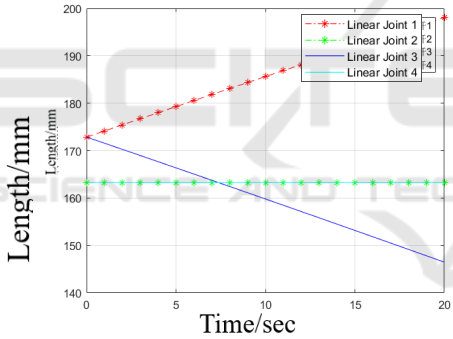

(b)

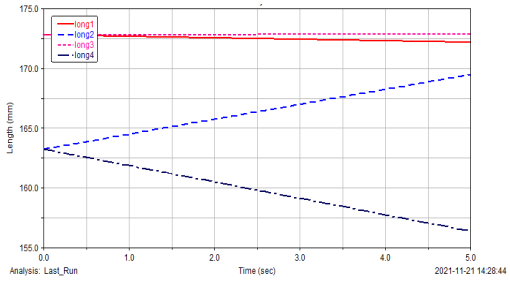

(c)

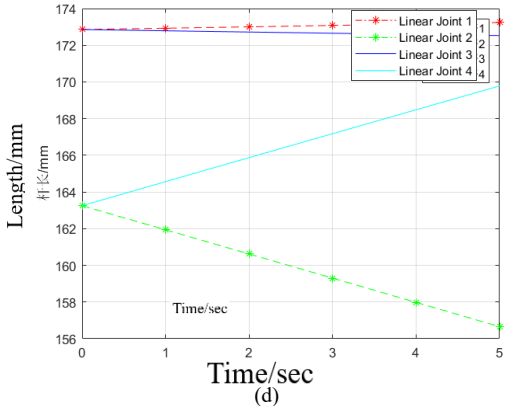

(d)

Figure 3: Robot inverse kinematics verification. (a)(c) ADAMS solution results under a certain spatial path (b)(d) Solution results of inverse kinematics model in a space path

4 4-RPUR PARALLEL ROBOT WORKSPACE

The coordinate search method based on inverse kinematics is adopted in this paper. According to the mechanism parameter design, it can be known that the maximum elongation L_{max} and the minimum elongation L_{min}, and the constraint condition of the linear actuator length during the mechanical movement is as follows:

$$L_{min} \le L \le L_{max} \tag{15}$$

The point when the driving linear actuators of the four limbs satisfy the linear actuator length constraint at the same time is the point that the mechanism can reach.

The specific search process is as follows: at the determined position to be studied, arbitrary pose parameters are given, and the length of the drive rod is calculated through the inverse kinematics of the robot in the previous chapter, to confirm whether it can be reached, the desirable point is marked, and the cycle is repeated in the previous step. The drawing workspace is shown in Figure 4. The approximate circular envelope surface of the working space of the robot moving platform in the figure also indirectly indicates that the robot has a coincident three-dimensional rotation center.

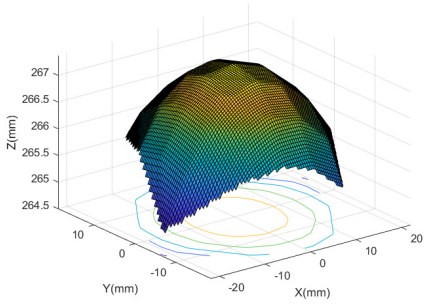

(a)

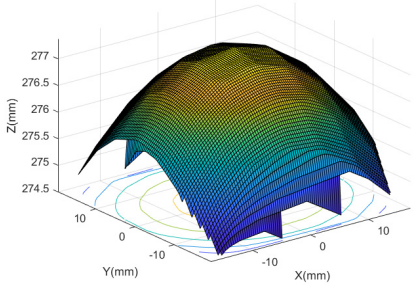

(b)

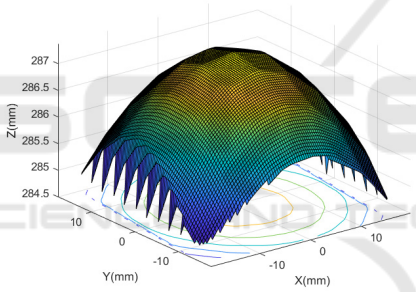

(c)

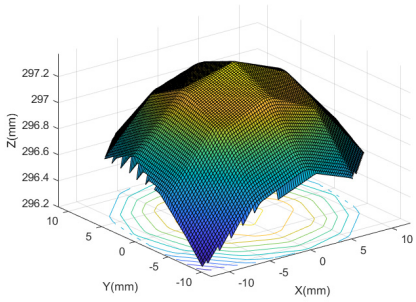

(d)

Figure 4: Workspace of 4-RPUR. (a) Move 160 Mm along the Z-Axis (B) Move 170 Mm along the Z-Axis (C) Move 180 Mm along the Z-Axis (D) Move 190 Mm along the Z-Axis.

5 ROBOT STRUCTURE DESIGN

According to the configuration design above, the robot's configuration is defined as 4-RPUR parallel configuration. Based on the relevant human dimension data, a parallel robot for medical-assisted rehabilitation of ankle joints is designed as follows. According to the structure and function of the robot, the robot can be divided into three parts, which are a fixed platform, a moving platform, and a limb part. The static and static platforms are equipped with mounting holes to fix the bone clips, the fixed platform includes a rapid assembly and disassembly structure of the robot, and the dynamic platform includes an adjustment structure to adapt to different sizes; The limb includes a drive rod and a hinge. The specific structure is shown in Figure 5:

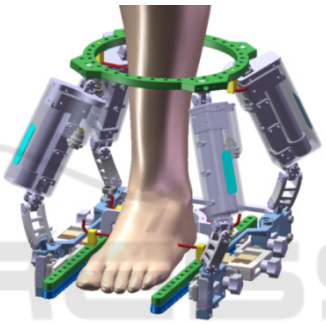

(a)

(b)

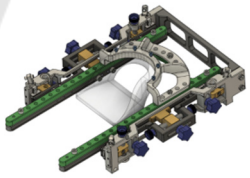

(c)

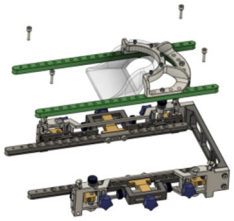

(d)

(e)

Figure 5: Robot structure design. (a) Ankle rehabilitation robot (b) Linear actuator (c-e) The moving platform of the rehabilitation robot.

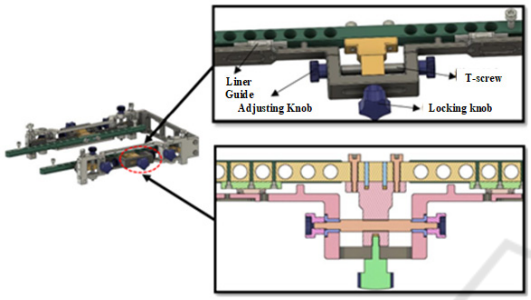

(a)

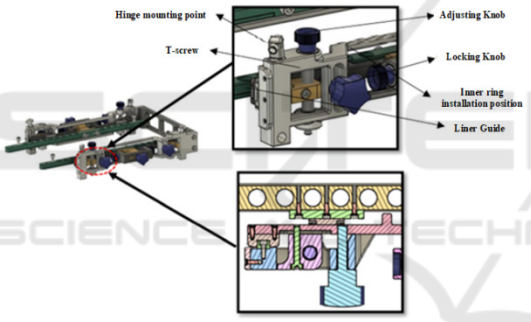

(b)

Figure 6: Robot adjusting structure. (a) The moving platform regulates the structure along the finger bone (b) The moving platform regulates the structure along the tibia.

The moving platform of the robot is mainly composed of two parts, which we call the inner ring and the outer ring. The inner ring is similar to the moving platform. The outer ring has a heel positioning device and an adjustment structure along two directions, which can adapt the size of the ankle bone, root bone, and talus of patients of different ages and genders to ensure that it coincides with the center of the ankle joint and reduces the passive slip of the ankle joint during exercise, as shown in figure 5 (c-e) and figure 6.

6 CONCLUSION

In this paper, a parallel mechanism 4-RPUR with a spatially determined coincidence three-dimensional rotation center is analyzed. The screw theory is applied to model the mechanism, and the degree of freedom of the robot is analyzed. At the same time, the screw is used to check the selected active joint and verify the correctness of the active joint selection. The kinematics model of the 4-RPUR parallel robot was deduced, the inverse kinematics analytical model of the robot was obtained and verified, and the working space was drawn. Finally, the structural design of the robot was completed.

ACKNOWLEDGMENTS

This work was financially supported by the Key-Area Research and Development Program of Guangdong Province (No.2020B0909020002) and Self-Planned Task (No.SKLRS202211B) of the State Key Laboratory of Robotics and System (HIT).

REFERENCES

Girone M, Burdea G, Bouzit M, et al. A Stewart Platform-Based System for Ankle Telerehabilit-ation[J]. *Autonomous Robots*, 2001,10(2):203-212. https://doi.org/10.1023/A:1008938121020

Kaufman KR, Irby SE, Mathewson J, et al. Energy-efficient knee-ankle foot orthosis: a case study[J]. *Prosthetics and Orthotics*, 1996, 8(3): 79-85. https://doi.org/10.1097/00008526-199600830-00003

Fan X, Li R, Li X, et al. (2-SPS+PU) &R Hybrid Ankle Joint Rehabilitation Robot and Kinematic Performance Analysis [J]. *Mechanical Science and Technology for Aerospace Engineering*, 2019, 38(07): 1035-1040. https://doi.org/10.13433/j.cnki.1003-8728.2019.20180277

Liu C, Zhang J J, Niu J Y, et al. Kinematic Performance of 4-DOF Generalized Spherical Parallel Mechanism for Ankle Rehabilitation [J/OL]. *Journal of Mechanical Engineering*, 2021, 57(21): 45-54. https://doi.org/10.3901/JME.2021.21.045

Han Y L, Yu J M, Song A G, et al. Parallel robot mechanism for ankle rehabilitation [J]. *JOURNAL OF SOUTHEAST UNIVERSITY (Natural Science Edition)*, 2015,45 (1): 45-50. https://doi.org/10.3969/j.issn.1001-0505.2015.01.009

Liu G Q, Gao J L, Yang S X, et al. The configuration of the ankle rehabilitation exercises parallel mechanism and its kinematics analysis[J]. *Development & Innovation of Machinery & Electrical Products*, 2005, 18(5): 13-15. https://doi.org/10.3969/j.issn.1002-6673.2005.05.005

Zhao T S, Yu H B, Dai J S. An ankle rehabilitation device based on a 3-RSS/S parallel mechanis-m[J]. *Journal of Yanshan University*, 2005, 29(6): 471-475. https://doi.org/10.3969/j.issn.1007-791X.2005.06.001

Yu R T, Fang Y F, Guo S. Design and performance analysis of a rope-driven parallel rehabilitation mechanism of ankle joint[J]. *Robot*, 2015, 37(1): 53-63. https://doi.org/10.13973/j.cnki.robot.2015.0053

Zhang X J, Liu G Q, He C Y, et al. A General Statement on the Ankle Rehabilitation Robot Based on Virtual Reality [J]. *Development & Innovation of machinery & electrical products*, 2006, 19(1): 29-31. https://doi.org/10.3969/j.issn.1002-6673.2006.01.011

Zuo S P, Dong M J, Li J F, et al. Configuration design and correction ability evaluation of a novel external fixator for foot and ankle deformity treated by U osteotomy[J]. *Medical & Biological Engineering & Computing*, 2020, 58(3). https://doi.org/10.1007/s11517-019-02103-w